JOURNAL OF GEOPHYSICAL RESEARCH, VOL. 108, NO. C3, 3069, doi:10.1029/2002JC001478, 2003

***Correction published 4 March 2004***

# Coupling between two inlets: Observation and modeling

P. L.-F. Liu,[1] S. Monserrat,[2,3] M. Marcos,[2,3] and A. B. Rabinovich[4]

Received 16 May 2002; revised 21 November 2002; accepted 4 December 2002; published 12 March 2003.

[1] The resonance coupling between two adjacent inlets is investigated. Field evidence of this natural phenomenon is found for two elongated inlets in the region of Ciutadella, Menorca Island, in the Western Mediterranean (Ciutadella and Platja Gran). To illustrate the fundamental features of the problem, analytical solutions for two rectangular inlets with constant depth are constructed and analyzed. The theoretical results mimic well the field data and demonstrate the resonance coupling characteristics of the inlet responses. The phenomenon is also examined with a numeric model so that the effects of real bathymetry can be considered. Numerical computations show the specific resonant features of local topography and the agreement between field data and numerical results is very good. *INDEX TERMS:* 4546 Oceanography: Physical: Nearshore processes; 4203 Oceanography: General: Analytical modeling; 4255 Oceanography: General: Numerical modeling; 4560 Oceanography: Physical: Surface waves and tides (1255); 4564 Oceanography: Physical: Tsunamis and storm surges; *KEYWORDS:* linear coupling, seiche oscillations, Balearic Islands, Western Mediterranean, rissaga waves

**Citation:** Liu, P. L.-F., S. Monserrat, M. Marcos, and A. B. Rabinovich, Coupling between two inlets: Observation and modeling, *J. Geophys. Res.*, *108*(C3), 3069, doi:10.1029/2002JC001478, 2003.

## 1. Introduction

[2] Ciutadella and Platja Gran are two elongated inlets located on the west coast of Menorca, on the Balearic Islands in the Western Mediterranean (Figure 1). Large sea level oscillations (up to 3 m trough-to-crest wave heights) are periodically observed in both inlets. These anomalous oscillations have been successfully linked to the passage of atmospheric pressure disturbances, generating long ocean waves on the continental shelf surrounding the islands that in turn, force the resonance response in the inlets [*Tintoré et al.*, 1988; *Monserrat et al.*, 1991; *Gomis et al.*, 1993; *Rabinovich and Monserrat*, 1998]. This phenomenon, locally known as "rissaga," is responsible for damage to boats and infrastructures in both locations, although the destructions are usually more severe in Ciutadella, where a harbor is located at the end of the inlet. The atmospheric forcing mechanism of the phenomenon was well established, but the energy transfer mechanism between the atmosphere and the ocean was still not because of the lack of field data on the shelf. For this reason, in the summer of 1997, a field experiment (LAST-97) was organized in the region of Ciutadella as a part of research collaboration between IMEDEA (Instituto Mediterráneo de Estudios Avanzados) at the University of the Balearic Islands and GIOC (Grupo de Ingeniería Oceanográfica y de Costas) at the University of Cantabria. A set of sea level and atmospheric pressure gauges were deployed and high-quality simultaneous sea level data on the shelf and inside both inlets were obtained. The preliminary examination of the field data has already given important information on the generation mechanism of rissaga waves and has led to the reconstruction of the transfer function between atmospheric disturbances and sea level responses [*Monserrat et al.*, 1998]. Furthermore, the data analysis has also revealed certain resonance interaction between Ciutadella and Platja Gran and it is likely that this interaction could be responsible for abnormal seiche oscillations in these inlets. The investigation of the resonance coupling between neighboring inlets constitutes the main goal of this paper.

[3] Two adjacent bays could interact with each other similar to the pendulums connected with a spring. *Nakano and Fujimoto* [1983] suggested the term "liquid pendulums" for such effects. The linkage mechanism between the bays is considered to be due to diffraction of waves radiated from the basins. The coupling mechanism could also be influenced by the wave reflection from a nearby coast, i.e., Mallorca Island (see Figure 1). However, in our case study, Ciutadella and Platja Gran are relatively close and Mallorca Island is located about 40 km away from the studied inlets. So, the diffraction mechanism is expected to dominate the interaction between inlets.

[4] The early interest in the coupling responses of two adjacent inlets (or bays) can be traced back to *Nakano* [1932], who studied the tsunami-induced oscillations in Koaziro Bay and Moroiso Bay in Japan. Field measurements revealed that a beat phenomenon existed in both bays. Nakano stated, "while one bay oscillates vigorously, the other rests more or less and vice versa" [also see *Murty*, 1977, p. 188]. Using the concept of conservation of energy

[1]School of Civil and Environmental Engineering, Cornell University, Ithaca, New York, USA.
[2]Grup d'Oceanografia Interdisciplinar/Oceanografia Física (GOIFis), IMEDEA (CSIC-UIB), Illes Balears, Spain.
[3]Departament de Física, Universitat de les Illes Balears, Palma de Mallorca, Spain.
[4]P. P. Shirshov Institute of Oceanology, Tsunami Laboratory, Moscow, Russia.


0148-0227/03/2002JC001478

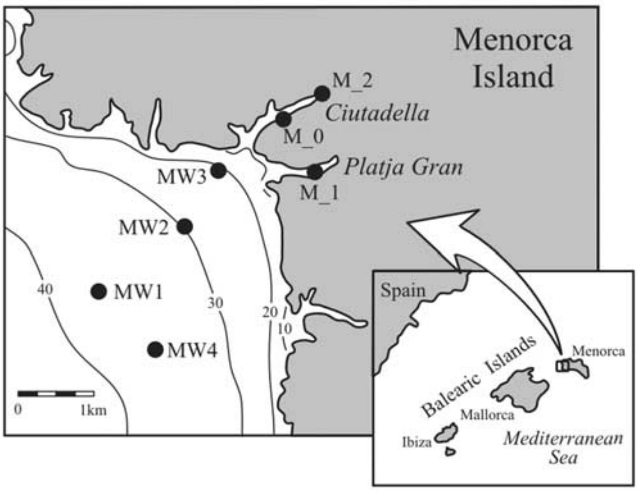


**Figure 1.** Inlets geometry and location of the instruments used for the present study off the western coast of Menorca, Balearic Islands, Western Mediterranean.

for two identical rectangular bays with constant depth, *Nakano* [1932] proposed a simplified analytical solution. The solution confirms the field observation, which is surprising and is perhaps erroneous. Since the rectangular bays are identical and parallel to each other and are perpendicular to a straight shoreline, the problem is symmetric as far as the bays are concerned; that is, there should not be any difference in the responses for these two bays. In an attempt to validate Nakano's analytic results and observations, *Nakano and Fujimoto* [1983] carried out a set of experiments. The experimental procedure was in this case nonsymmetric and can be described briefly as follows. One of the identical inlets was resonated first with the other inlet mouth closed. After the quasi-steady state was reached, the mouth of the second bay was opened suddenly. The observations were made in both bays, and the beat phenomenon was identified during the transient. More recent research on the coupled bay system has been focused on the so-called Y-shaped model, in which two bays merge into one (the "stem") before reaching the sea [e.g., *Aida et al.*, 1972; *Arai and Tsuji*, 1998]. Numerical simulations have been carried out to identify the resonance modes for the Y-shaped bay system, in which the stem is an integrated part of the system.

[5] Referring to Figure 1, Ciutadella and Platja Gran are closer to two parallel rectangular inlets than to a Y-shaped bay system. On the basis of the shallow-water wave theory and using a matched asymptotic method we will seek for analytical solutions for the responses in two adjacent rectangular inlets with constant depth. Although the geometry is similar to those used by Nakano and his associates, they were mainly concerned with the transient problem and their approach is quiet different from the one to be used here. It is our hope that the analytical solutions will not only shed some lights on the interpretation of the field observations in Ciutadella region but also provide some information on the effects of the ratio of the inlet lengths and the distance between two inlets.

[6] To further enhance our understanding of the specific coupling responses for Ciutadella and Platja Gran, numerical solutions of the linear shallow-water equations are also obtained by using the real bathymetry. With the observed data as incident wave conditions, wave spectra inside the inlets are estimated. The agreement between observations and numerical simulations is very good and the numerical results are used for a final interpretation of the significant peaks in the measured spectra and admittance functions in the inlets.

[7] The paper is organized as follows. In section 2 the experiment LAST-97 and available field data are described and evidences of resonance coupling between the nearby inlets, Ciutadella and Platja Gran, are demonstrated. In section 3 the analytical solutions of resonance oscillations in two adjacent narrow rectangular inlets are constructed. With a proper choice of parameters, the analytical solution is used to explain the observed resonance coupling of Ciutadella and Platja Gran inlets. The numerical modeling of resonance oscillations in these inlets is presented in section 4. Finally, in section 5 some concluding remarks are made with suggestions for future study.

## 2. Field Observation and Evidences

[8] During the LAST-97 field experiment from June to September 1997, four sea level recorders (bottom pressure gauges MW1, MW2, MW3, and MW4) were deployed on the shelf in front of Ciutadella. As shown in Figure 1, two more pressure gauges were located inside the Ciutadella Inlet, one near the middle (M_0) and the other one close to the end of the inlet (M_2), and the last pressure gauge was installed near the middle of the neighboring inlet of Platja Gran (M_1). All bottom pressure gauges recorded continuously for 30 s intervals and stored the data with a sampling interval $\Delta t$ = 1 min.

[9] Several rissaga episodes occurred during the experimental period (see *Monserrat et al.* [1998]); however, in this paper we will not consider these episodes and shall, instead, focus on the effects of coastal planeform (i.e., the topography) on the inlet responses. To achieve this objective, we have chosen a background period of relatively weak inlet oscillations from 0400h of 29 July to 1600h of 30 July (36 hours) for thorough analysis and discussion. The significant wave heights inside the inlets during this period are in the order of magnitude of few centimeters and the measured wave heights on the shelf are one order of magnitude less.

[10] The spectral contents have been estimated for each instrument, inside Ciutadella and Platja Gran inlets and on the shelf. A Kaiser-Bessel window of 512 points with half-window overlapping was used for all the computations [*Emery and Thomson*, 1997], initially resulting in 14 degrees of freedom (dof). The presented spectra have been additionally smoothed so that the number of degrees of freedom is increased with increasing frequency. This leads to a sliding scale where the lowest frequency range uses 14 dof, but the next frequency band averages the spectra of three adjacent frequencies to give 42 dof, the next averages the spectra of five adjacent frequencies to give 70 dof, and so on. The computed spectra with the corresponding 95% confidence limits are shown in Figure 2. The low frequency components of the spectra are very similar in both inlets and on the shelf. (Here only the MW4 spectrum is shown;

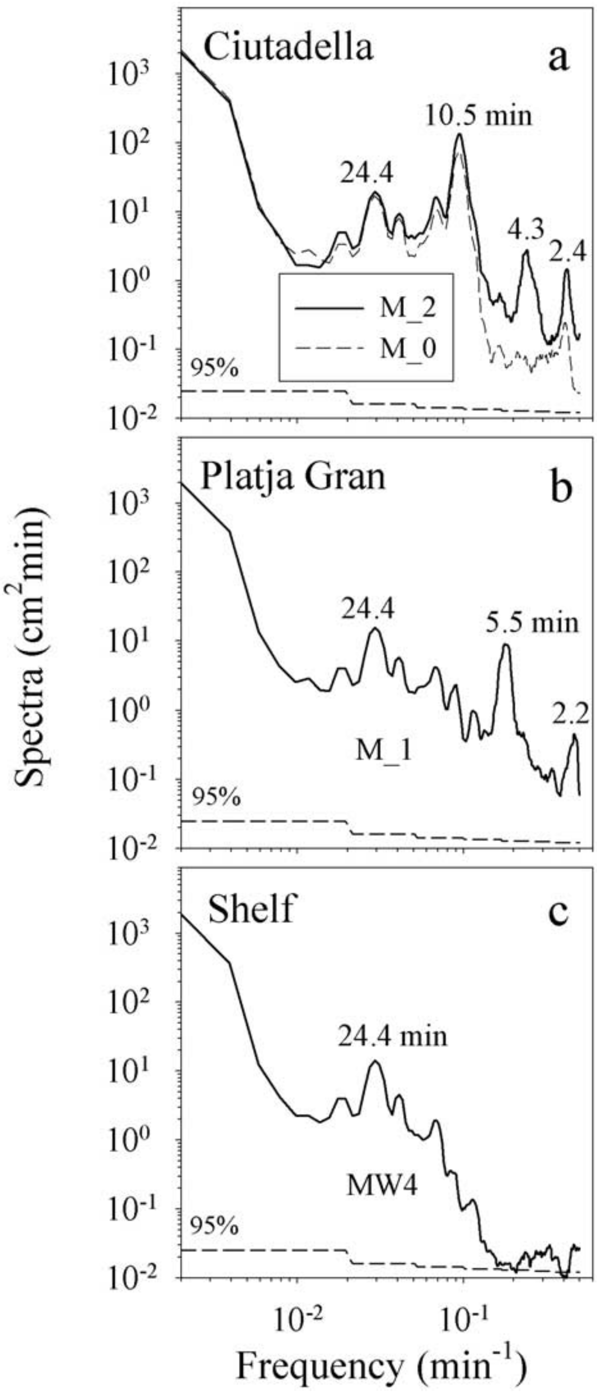


**Figure 2.** Sea level spectra for Ciutadella (a), Platja Gran (b), and Station MW4 located on the shelf (c). Solid line in Figure 2a corresponds to M_2 instrument, and dashed line corresponds to M_0. The periods (in minutes) of the major peaks are indicated. (See Figure 1 for the positions of the instruments.)

however, similar behavior has been also observed for other instruments). In particular, the prominent peak at the period of 34.1 min and other low-frequency peaks (24.4 min, 14.6 min) are observed in every instrument. As suggested by *Monserrat et al.* [1998], these peaks are related to the shelf resonant characteristics. These shelf resonant frequencies exist in the inlets without any amplification since they are well below the fundamental resonant frequencies of the inlets.

[11] The spectra for the three sites inside the inlets differ significantly from the spectra of the shelf instruments at high frequencies (>0.08 min$^{-1}$), reflecting the influence of the respective inlets. A very energetic spectral peak with a period of 10.5 min, which is related to the fundamental (Helmholtz) mode of Ciutadella Inlet (see *Rabinovich et al.* [1999]), is the main feature of the spectra at M_0 and M_2. The energy at Station M_2, being located near the end of the inlet, is greater than that at M_0, which is near the middle of the inlet. This is related to the shape of the fundamental mode, which has the only one node at the inlet entrance [*Wilson*, 1972]. Lower spectral peaks are also observed at wave periods of 4.3 min and 2.4 min. Note that the peak at 4.3 min is significant only at Station M_2. This peak becomes rather weak in the M_0 spectrum probably because the respective instrument is located very close to the nodal line of this mode. Therefore this resonance peak is likely the first mode of this inlet that normally has two nodes: one at the inlet entrance and the other at a distance of approximately two thirds of the inlet length from the entrance [*Wilson*, 1972]. The Platja Gran spectrum (Figure 2b) shows a peak at the fundamental (Helmholtz) mode with a period of 5.5 min, which is less energetic than that in Ciutadella but is still very well defined. The spectral peak of another mode with a period of 2.2 min is also well defined but with a much smaller magnitude. Since M_1 is located near the middle of the inlet, the peak associated with the first mode should not be seen (the situation is similar to that for Station M_0 in Ciutadella Inlet), so this peak (2.2 min) is apparently related to the second mode of Platja Gran Inlet. These assumptions are supported by numerical computations made by *Rabinovich et al.* [1999]. By using a coarse resolution finite difference numerical model and random perturbations of the red noise type as the external forcing, these authors computed the spectra of the calculated oscillations at different points inside the inlets. The fundamental modes for Ciutadella and Platja Gran were found for 11.1 min and 6.1 min. The first modes were 4.7 min (Ciutadella) and 3.6 min (Platja Gran), respectively, when they are computed at the end of the inlets. They were absent near the middle of the inlets. In the following sections they will be further investigated with the help of analytical solutions and numerical results.

[12] Shelf resonance characteristics, affecting all instruments, may be easily removed from the spectra at the inlet sites by dividing the spectra by the spectrum at one of the instruments on the shelf. The square root of this ratio may be considered as a good estimation of the inlet admittance function, i.e., as the relative amplification of the waves, arriving from the shelf, inside the inlet. Instrument MW4 is selected as the representative of shelf oscillations, although it is located relatively far away from the inlet entrances (see Figure 1). Instrument MW3 could be an alternative choice, however; being very close to the inlet entrance, it is affected by radiated waves from the inlets at resonance frequencies.

[13] On the basis of the field data the amplification functions were computed for both instruments at Ciutadella and for the one at Platja Gran (Figure 3). The admittance

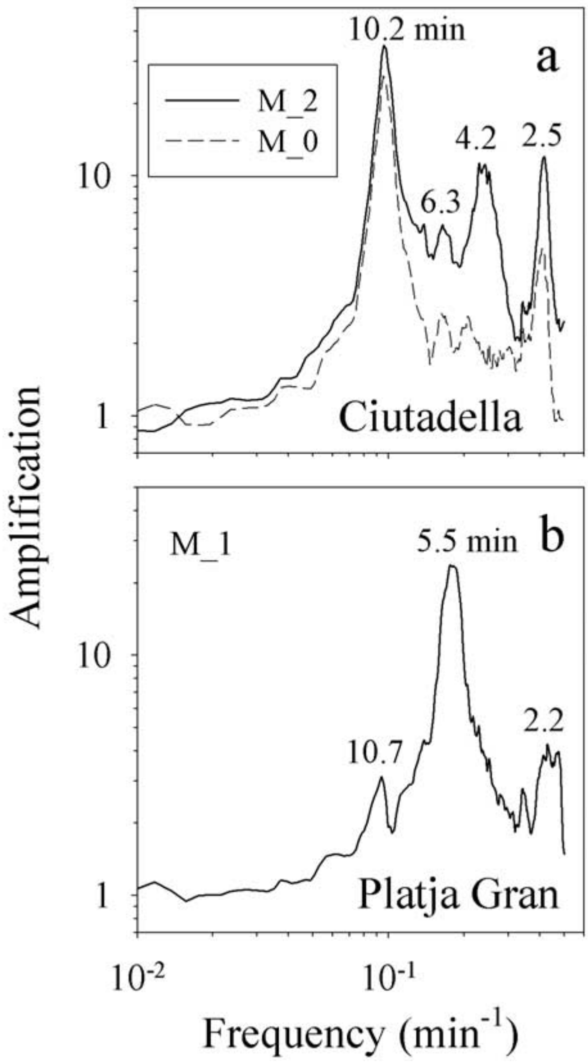


**Figure 3.** Admittance functions for Ciutadella (a) and Platja Gran (b). Solid line in Figure 3a corresponds to M_2 instrument, and dashed line corresponds to M_0. The periods (in minutes) of the major peaks are indicated.

resonant peaks for both inlets appear to be sharper than those in the spectra, although the respective frequencies are slightly different. These small shifts are not surprising because the spectrum on the shelf is not a constant. The computed functions resemble the admittance functions expected for a harmonic oscillator identifying the major peaks as the fundamental and higher modes for each inlet. However, in addition to the inlet's resonant modes, several secondary but clear peaks are also apparent. They seem to be located at the frequencies coinciding with the resonant frequencies of the adjacent inlet, suggesting the resonance coupling between two inlets. To better understand the nature of these additional response peaks in these inlets, a simple analytical model is developed in the following section.

## 3. Coupling of Harbor Resonance in Two Inlets

[14] In this section we investigate the natural resonance phenomena described in the previous section with a simple system so that analytical solutions can be constructed. Consider two rectangular inlets with the following dimensions, $2b_1 \times l_1$ and $2b_2 \times l_2$ respectively. As shown in Figure 4 the inlets are located along a straight coastline, coinciding with the $y$ axis. The $x$ axis is pointing in the offshore direction. For simplicity, the water depth inside and outside the inlets is kept as a constant, $h$. Furthermore, the coastline and the sidewalls of the inlets are assumed to be vertical and perfect reflecting. The distance between two inlets is denoted as $d$ (see Figure 4). The analysis that follows is linear. This is justifiable so, based on the field data, the incident wave amplitude is always less than a few centimeters. Considering the wave period of the highest resonance mode shown in Figure 3, i.e. 2.2 min, as the characteristic wave period, the corresponding wavelength in the water depth of 30 m is about 2 km. Therefore the wave system, even under the resonance condition, is linear.

[15] Thus for the analytical analysis the incident waves are characterized by the wave amplitude, $a$, and the wave frequency, $\omega$, and the free surface displacement for the normal incident wave train can be expressed as $\zeta_i = ae^{-i(kx+\omega t)}$, where $k = \omega/\sqrt{gh}$ is the wave number with $c = \sqrt{gh}$ being the phase speed. In order to find the analytical solutions, the following assumptions and simplifications are made. First, the inlets are assumed to be very narrow, i.e. $2b_1/l_1 \gg 1$ and $2b_1/l_1 \ll 1$. Second, the length of the inlets is in the same order of magnitude of the incident wavelength, which is very long in comparison with the water depth.

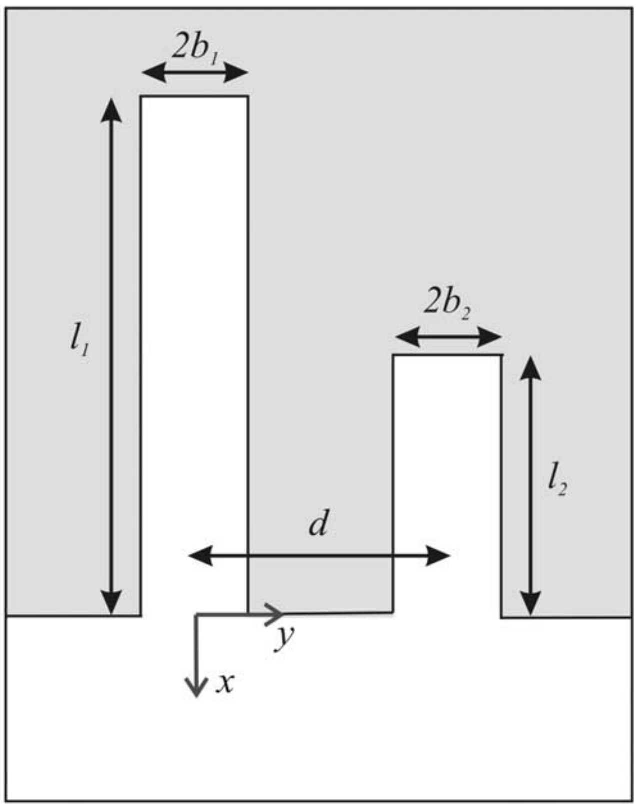


**Figure 4.** Two inlets geometry and used dimensions.

[16] Adopting the assumptions that the long wave system is linear, a matched asymptotic method is employed to obtain solutions. Rewriting the incident wave as

$$\zeta_i = \eta_i(x)e^{-i\omega t} = ae^{-ikx}e^{i\omega t}, \tag{1}$$

we assume that the wave responses in the inlets and in the ocean satisfy the linear wave equation,

$$\frac{\partial^2\zeta}{\partial t^2} + gh\left(\frac{\partial^2\zeta}{\partial x^2} + \frac{\partial^2\zeta}{\partial y^2}\right) = 0. \tag{2}$$

[17] The wave field in the ocean, sufficiently far away from the inlets, can be written as

$$\zeta_o = \eta_o e^{-i\omega t}; \quad \eta_o = 2a\cos kx + \frac{\omega Q_1}{2g}H_0^{(1)}(kr_1) + \frac{\omega Q_2}{2g}H_0^{(1)}(kr_2), \tag{3}$$

in which $r_1$ and $r_2$ measure the distance from the mouth of inlet 1 and 2, respectively, i.e.,

$$r_1 = \sqrt{x^2 + y^2}, \text{ and } r_2 = \sqrt{x^2 + (y-d)^2},$$

$H_0^{(1)}$ is the Hankel function of the first kind of order zero, $Q_1$ and $Q_2$ represent the fluxes across the inlet entrance, respectively. From equation (3) it is clear that the coastline has been assumed to be perfectly reflective so that the first term in the expression represents a standing wave. We also remark here that the Hankel function of the second kind of order zero is also the solution to the governing equation (2). However, since $H_0^{(1)}(kr_{1,2})$ becomes $\exp(ikr_{1,2})/\sqrt{kr_{1,2}}$ as $kr_{1,2} \to \propto$ and represents outgoing waves, it is the only admissible solution. The inner expansion of the far-field solution in the ocean can be readily written as

$$\eta_o \approx 2a + \frac{\omega Q_1}{2g}\left(1 + \frac{2i}{\pi}\ln\left[\frac{\gamma kr_1}{2}\right]\right) + \frac{\omega Q_2}{2g}H_0^{(1)}(kd), kr_1 \ll 1 \tag{4}$$

$$\eta_o \approx 2a + \frac{\omega Q_2}{2g}\left(1 + \frac{2i}{\pi}\ln\left[\frac{\gamma kr_2}{2}\right]\right) + \frac{\omega Q_1}{2g}H_0^{(1)}(kd), kr_2 \ll 1 \tag{5}$$

where ln $\gamma$ = Euler's constant = 0.5772157....

[18] In the inlets, because of their narrowness, the wave fields consist of two progressive wave trains propagating in the opposite direction along the inlet. Since the end walls of these inlets are also perfectly reflective, the free surface displacements inside the inlet and far away from the entrance can be expressed as

$$\zeta_{bj} = \eta_{bj}(x)e^{-i\omega t}; \; \eta_{bj} = 2a\Re_j\cos k(x + l_j), \tag{6}$$

where $j$ = 1, 2 for inlet 1 and 2 respectively. The inner expansion of the wave field in the inlet toward the entrance can be obtained by requiring $kx \to 0$,

$$\eta_{bj} \approx 2a\Re_j[\cos kl_j + (\sin kl_j)kx]. \tag{7}$$

[19] To connect the wave field in the ocean and those in the inlets, one needs to find the approximate solutions in the vicinity of inlet entrance. Because the width of the inlet is assumed to be small in comparison with the wavelength, flow motions near the inlet entrance (the near field) are governed by the Laplace equation. Therefore the near-field problem is that of a potential flow past a right-angled estuary. The solution can be obtained by the technique of conformal mapping. The details of the solution finding procedure are given by *Mei* [1989, p. 199–201] and will not be repeated here. Only the outer expansions of the near field solutions are given here

$$\eta_{ej} = M_j\frac{\pi x}{2b_j} - M_j\ln\left(\frac{e}{2}\right) + C_j, \qquad x < 0 \tag{8}$$

$$\eta_{ej} = M_j\ln\left(\frac{\pi r}{2b_j}\right) + C_j, \qquad x > 0 \tag{9}$$

in which $\zeta_{ej} = \eta_{ej}e^{-i\omega t}$ represents the free surface displacement in the entrance of the $j$th inlet. Note that in equation (8) ln $e$ = 1. Matching of the inner and outer solutions on the inlet sides and the ocean side yield a set of eight linear algebraic equations for eight unknown coefficients, $M_j$, $C_j$, $\Re_j$, and $Q_j$. After some lengthy, but straightforward manipulations, $\Re_j$ can be found as

$$\Re_j = \frac{U_j}{V_j}, \quad j = 1, 2 \tag{10}$$

with

$$U_j = \cos kl_m + \frac{2kb_m}{\pi}\sin kl_m\ln\left(\frac{2\gamma kb_m}{\pi e}\right) - ikb_m\sin kl_m\left(1 + H_0^{(1)}(kd)\right) \tag{11}$$

$$\begin{aligned} V_j = &\left[\cos kl_j + \frac{2kb_j}{\pi}\sin kl_j\ln\left(\frac{2\gamma kb_j}{\pi e}\right) - ikb_j\sin kl_j\right] \\ &\times\left[\cos kl_m + \frac{2kb_m}{\pi}\sin kl_m\ln\left(\frac{2\gamma kb_m}{\pi e}\right) - ikb_m\sin kl_m\right] \\ &+ kb_jkb_m\sin kl_j\sin kl_m\left[H_0^{(1)}(kd)\right]^2 \end{aligned} \tag{12}$$

in which $m$ = 1 or 2, but $m \neq j$. Since the solutions for inlet 1 and inlet 2 are symmetric, the rest of analyses will be focused on inlet 1. The amplification factor, $\Re_1$, becomes much simpler if the second inlet does not exist, i.e., $b_2$ =0. Thus

$$\Re_1 = \frac{1}{\cos kl_1 + \frac{2kb_1}{\pi}\sin kl_1\ln\left(\frac{2\gamma kb_1}{\pi e}\right) - ikb_1\sin kl_1}. \tag{13}$$

[20] The above amplification factor can be rewritten approximately in the neighborhood of the $n$-th ($n$ = 0, 1, 2,...) resonant mode as [*Mei*, 1989]:

$$\Re_1 \approx \frac{1}{(-1)^{n+1}\left[(k - \tilde{k}_n)l_1 + ik_nb_1\right]} \tag{14}$$

where

$$\tilde{k}_n = k_n\left[1+\frac{2b_1}{\pi l_1}\ln\left(\frac{2\gamma k_n b_1}{\pi e}\right)\right]; \quad k_n l_1 = \left(n+\frac{1}{2}\right)\pi, \quad n = 0,1,2,\ldots \tag{15}$$

[21] The peak responses occur at $k = \tilde{k}_n$ since $\tilde{k}_n$ are always less than $k_n$ the shifting of the resonant wave numbers (or frequencies) is always toward the lower wave number (or frequency). The peak values of the resonant response are simply

$$|\Re_1|_{\max} = \frac{1}{k_n b_1} = \frac{l_1/b_1}{(n+1/2)\pi}. \tag{16}$$

Thus the heights of the successive resonant peaks decreases with the mode number $n$.

[22] Similar analysis can be carried out when the second inlet exists. The result is

$$\tilde{k}_n = k_n\left[1+\frac{2b_1}{\pi l_1}\ln\left(\frac{2\gamma k_n b_1}{\pi e}\right)+\Delta\right];$$

$$\Delta = -\frac{b_1}{l_1}\frac{k_n b_2 \sin k_n l_2\left[\left(1-J_0^2+Y_0^2\right)(P_2+k_n b_2\sin k_n l_2 Y_0)-P_2(1+J_0)\right]}{\left[P_2(P_2+k_n b_2 \sin k_n l_2 Y_0)+(k_n b_2 \sin k_n l_2)^2(1+J_0)\right]}; \tag{17}$$

$$P_2 = \cos k_n l_2 + \frac{2k_n b_2}{\pi}\sin k_n l_2 \ln\left(\frac{2\gamma k_n b_2}{\pi e}\right)$$

Owing to the appearance of the second inlet, a further shift of peak responses, $k_n\Delta$, is introduced. In the formula, the arguments of the Bessel functions of first kind, $J_0$ and of second kind, $Y_0$ of order zero are $k_n d$. The sign and the magnitude of the additional shift depend on $k_n I_{12}$, $k_n b_2$, and $k_n d$.

[23] The amplification factors, $|\Re_1|$ and $|\Re_2|$, can be readily evaluated, once the wave parameters and the geometric parameters are specified. To explore the field situation described in the previous section (see Figure 1), the following values are used:

$$l_1 = 1000m, l_2 = 500m, 2b_1 = 2b_2 = 100m, d = 250m, \quad h = 5.5m. \tag{18}$$

Therefore the corresponding dimensionless parameters are

$$\frac{l_1}{l_2} = 2.0, \frac{b_1}{l_1} = 0.05, \frac{b_2}{l_2} = 0.1, \frac{d}{l_1} = 0.25. \tag{19}$$

In Figure 5, the amplification factors for both inlets are plotted against $kl_1$. In the same figure the amplification factor for each inlet in the absence of the other inlet is also plotted. The effects of resonance coupling of two inlets are quite clear. The resonance frequencies of each inlet are shifted slightly due to the appearance of the other inlet. The magnitudes of the peak responses are also modified. Additional sharp peaks appear in the amplification factors and these peaks correspond to the resonance frequencies of the other inlet.

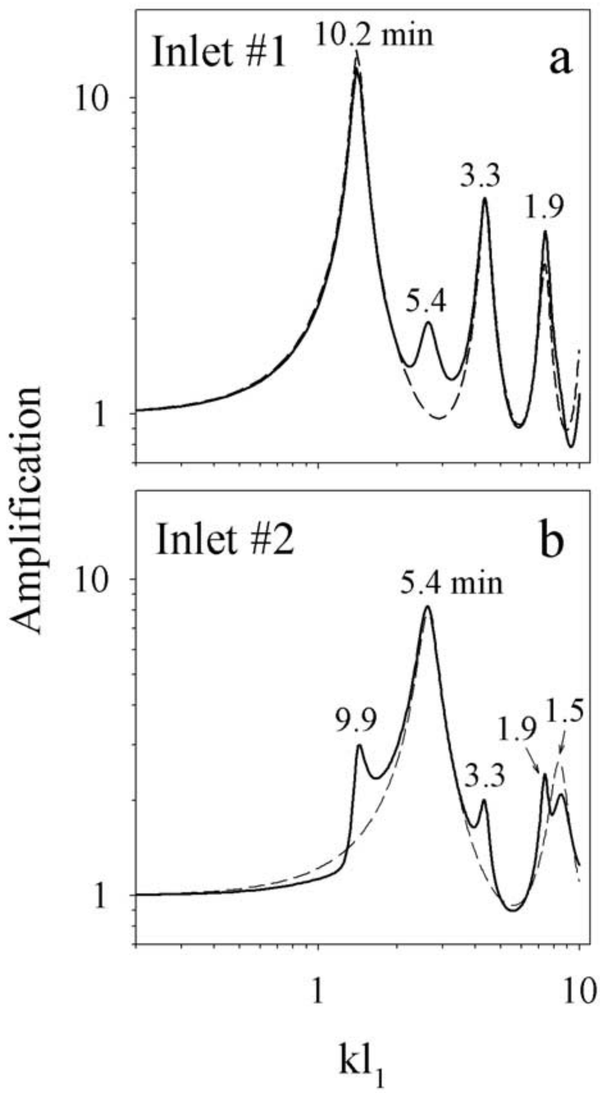


**Figure 5.** Amplification factors for Inlet 1 (a) and Inlet 2 (b), when both inlets are present (solid lines) and only one (first or second) exists (dashed lines). The period (in minutes) of the resonant modes for geometric parameters of Ciutadella and Platja Gran inlets are indicated.

[24] On the basis of the results shown in Figure 5 the fundamental resonant mode for Inlet 1 occurs at $kl_1$ = 1.4 and the corresponding resonance period, which can be roughly calculated from $T = 2\pi/(k\sqrt{gh})$, is 10.2 min. The first resonant mode for Inlet 1 is at $kl_1$ = 4.35 and the period is 3.3 min. A small response peak appears between the fundamental and the first resonant mode at $kl_1$ = 2.7 and $T$ = 5.4 min, which also corresponds to the fundamental resonant mode of Inlet 2. The second resonant mode for Inlet 1 occurs at $kl_1$ = 7.4 and $T$ = 1.9 min. The amplification factor for the second inlet shows similar characteristics; sandwiching the fundamental resonant mode of Inlet 2, there are two small peaks corresponding to the fundamental and first resonant modes of Inlet 1. The first resonant mode of Inlet 2 occurs at $kl_1$ = 9.4 and $T$ = 1.5 min, which is very close to the second resonant mode of Inlet 1 as shown in Figure 5b. The second resonant mode of Inlet 2 is at $kl_1$ = 15.7 and $T$ = 0.91 min.

[25] Since the parameters used in calculating the results shown in Figure 5 have been intentionally chosen to be representative of Ciutadella (as Inlet 1) and Platja Gran (as Inlet 2), it is satisfying to observe that the theoretical results (Figure 5) mimic the field data (Figure 3) very well, in terms of the fundamental characteristics of the responses. The exact matches in terms of magnitudes for peak responses and the resonance frequencies should not be expected due to the simplifications of bathymetry and shoreline configuration in the analytical solutions. It is well known that when the depth and/or the width of the inlet are not constant, the ratios $T_n/T_0$ ($T_0$ being the period of the fundamental mode and $T_n$ the period of the nth mode) may considerably depart from those of the rectangular inlet with constant depth, for which $T_n/T_0 \approx 1, 1/3, 1/5\ldots$. For example, $T_n/T_0 = 1, 0.409, 0.259$ for a rectangular inlet with a semi-parabolic bottom ($h(x) = h_0[1-x^2/l^2]$) (see, e.g., *Wilson*, 1972, Table II). These modified ratios are much closer to the measured values, in particular for Ciutadella Inlet.

[26] The coupled inlet responses depend on the parameters used. The ratio of the inlet lengths, $l_2/l_1$ and the distance between two inlets, $d/l_1$ play key roles. As an example, consider the situation where the geometry of these two inlets remains the same as that described in equations (18) and (19), except that the distance between them is allowed to vary. The response curves for Inlet 1 and Inlet 2 with $d/l_1$ = 0.1, 0.25, and 2.0 are plotted in Figure 6. Since the inlet configuration has not been modified, the resonant frequencies of each inlet also remain unchanged. As two inlets become closer the magnitudes of responses become larger. It is interesting to observe that because the second resonant mode of Inlet 1 is very near the first resonant mode of Inlet 2, the response in Inlet 2 is significantly enhanced in the vicinity of these two resonance modes as two inlets becoming very close to each other (e.g., $d/l_1$ = 0.1). As the distance between the inlets increases, the influence of one inlet to the other diminishes as expected. When $d/l_1 > 5.0$ the behaviors of these two inlets are almost independent of each other for the present case.

[27] In Figure 7 the response curves are presented for the cases where the distance between two inlets is fixed, $d/l_1$ = 0.25, but the length of Inlet 2 is allowed to vary. In these figures three different lengths are shown, $l_2/l_1$ = 0.2, 0.5, and 1.0. Since the length of Inlet 1 has not been altered, the resonant frequencies of Inlet 1 remain the same for all three cases. However, the resonant modes for Inlet 2, in terms of $kl_1$ change significantly. For the case of $l_2/l_1$ = 0.2, the fundamental resonance mode of Inlet 2 almost coincides with the second resonant mode of Inlet 1, resulting a very wide peak, implying that the coupled inlets can be resonated much easier within this particular range of frequencies. As $l_2/l_1$ becomes one, two inlets have identical length with identical resonant frequencies. The peak responses are further amplified; the maximum response at the first mode in Inlet 1 is 180, while it is about 83 in Inlet 2. The difference is the result of different inlet width, i.e., $b_1/l_1$ = 0.05 and $b_2/l_2$ = 0.1 The responses would have been identical in both inlets if the widths were the same. This conclusion is fully expected, but is very different from that of *Nakano* [1932]. If the incident wave is somewhat energetic at the resonance mode, the wave action could be very violent under this circumstances; a nonlinear theory is required.

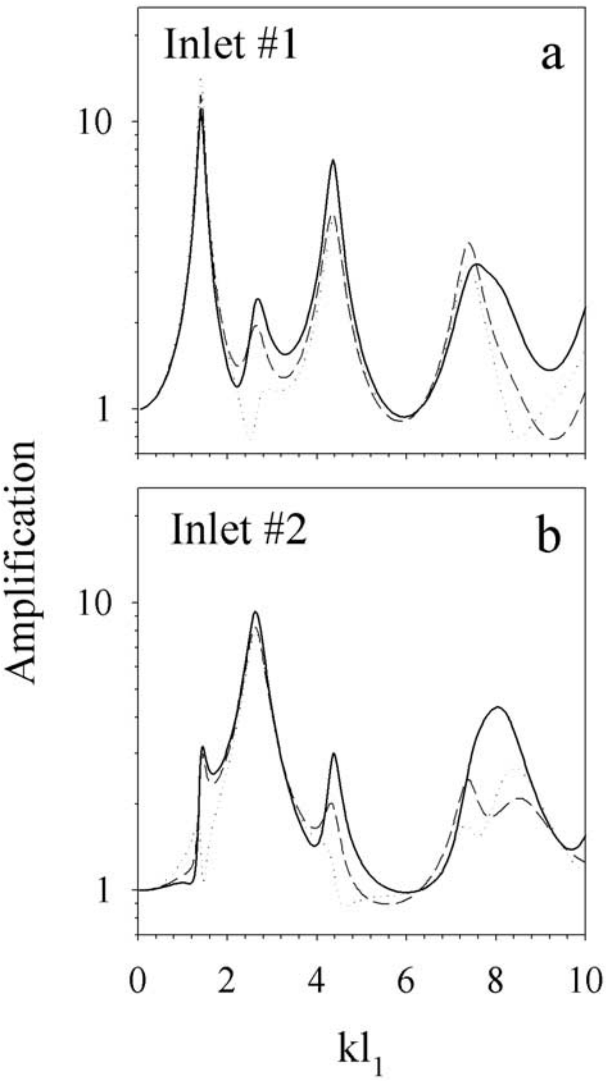


**Figure 6.** The response curves for Inlet 1 (a) and Inlet 2 (b) for different values of the non-dimensional parameter $d/l_1$ = 0.1 (solid), $d/l_1$ = 0.25 (dashed) and $d/l_1$ = 2.0 (dotted).

## 4. Numerical Model

[28] Although the analytical model developed in the previous section has provided insights into the resonance coupling of a two-inlet system, it has limitations due to the simplification of real shape and bathymetry of the inlets. In this section a two-dimensional finite difference model based on the linear shallow-water wave equations is used to numerically simulate the inlet responses in Ciutadella and Platja Gran with the real bathymetry and topography data [*Grupo de Ingeniería Oceanográfica y de Costas* (*GIOC*), 1990]. The model does not include the effects of the Earth's rotation nor of bottom friction. The Coriolis acceleration can justifiably be ignored because the focus is on wave periods much shorter than the local inertial period. Bottom

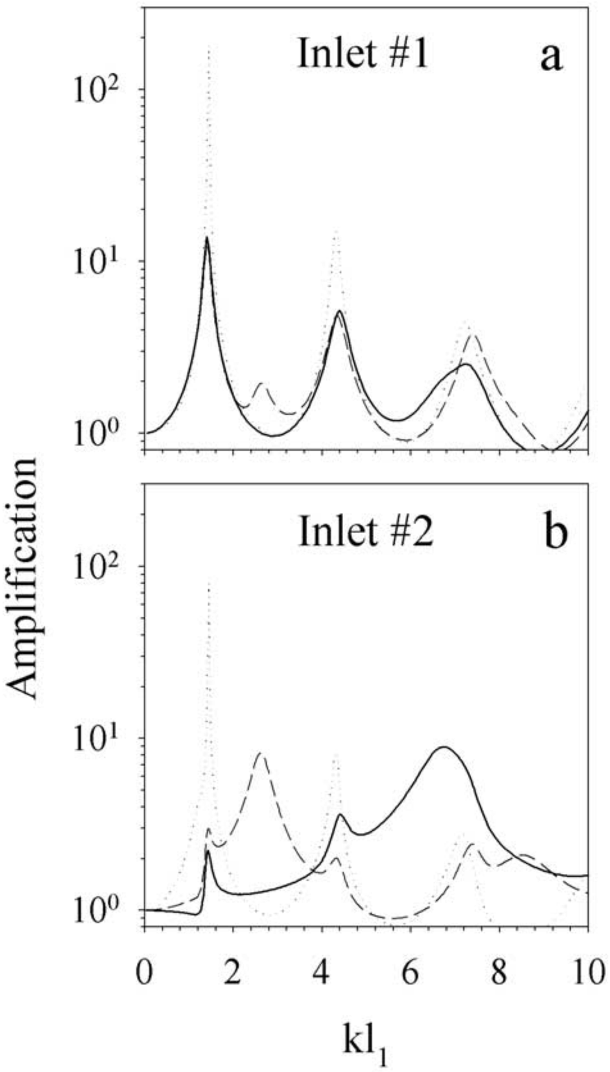


**Figure 7.** The response curves for Inlet 1 (a) and Inlet 2 (b) for fixed $d/l_1$ = 0.25 and $l_2/l_1$ = 0.2 (solid), $l_2/l_1$ = 0.5 (dashed) and $l_2/l_1$ = 1.0 (dash-dotted).

friction may be ignored since the main effect of limiting the resonant response in the inlets is due to seaward radiation of energy from the inlet mouths. The model integrates the depth-averaged equations of continuity and momentum which are written on a staggered grid (Arakawa C). The computational domain and the bathymetry are shown in Figure 8. A uniform grid with the spatial resolution $\Delta x = \Delta y$ = 10 m is used, resulting in 119 × 199 points. According to the Courant criterion the time step is chosen to be $\Delta t$ = 0.5 s. The sea level data measured at MW4 are used as input data on all the grid points along the lower boundary of the computational domain. The values for each time step are obtained by interpolating the field time series data. A radiation boundary condition is applied along the right-hand side of open boundary. Along the coastline the full reflecting boundary condition is employed.

[29] Figure 9 shows the computed spectra for the two inlets. Two points are selected in each inlet; one is near the end and the other is near the middle of the inlet. The middle points are close to the positions of M_1 in Platja Gran and M_0 in Ciutadella inlets (see Figure 8). The measured spectra shown in Figure 2 (for M_2 and M_1) are also included for comparison. The agreement between the measured and computed spectra is quite reasonable. The model properly simulates the frequency and magnitude of the fundamental mode (10.5 min) as well as the higher modes in Ciutadella (Figure 2a), although the energy of the simulated higher modes is slightly less in the observations. The first mode (4.3 min), as expected, is only observed at the end of the inlet. The fundamental mode at Platja Gran (5.5 min) is also well simulated; it appears at both locations in the inlet, with slightly more energy at the point located near the end of the inlet. An additional peak at a period of 3.7 min (not apparent in the observational spectrum) is clearly identified in the numerical results at the end of the inlet. However, this peak is absent, or at least much less evident, when plotting the results for a computational point close to the actual position of M_1 instrument, suggesting that this peak is indeed related to the first mode of Platja Gran Inlet. This confirms our discussions in section 2 that the resonance peak at 2.2 min period corresponds to the second resonance mode of this inlet. The obtained ratio $T_n/T_0$ for the first mode is 0.660, which is much greater than the corresponding value for the constant depth and width case (0.333) and also greater than that for the semiparabolic

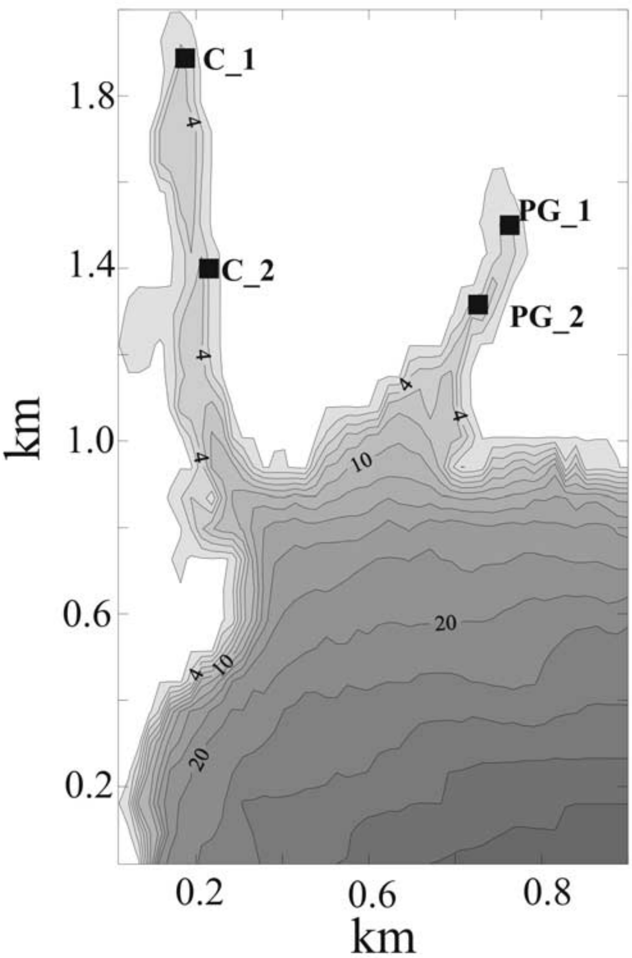


**Figure 8.** Model domain and bathymetry. The points where the spectra have been computed are marked.

depth (0.409). The higher ratio, however, is justifiable for a wider open mouth bay [see *Wilson*, 1972, Table II], as is the case of Platja Gran. These results are similar to those found by *Rabinovich et al.* [1999] who numerically computed the significant resonant peaks in Ciutadella and Platja Gran inlets using a coarser bathymetry for the computational area and red noise as the input function on the open boundary.

[30] To investigate better the coupling phenomenon, the amplification factor for both inlets is also computed by dividing the inlet spectra by the forcing. Results for two computational points close to the positions of M_2 (C_1) in Ciutadella and M_1 (PG_2) in Platja Gran are shown in Figure 10. For comparison the results for a single inlet (artificially closing the adjacent inlet) are also plotted at C_1 and PG_2 (dashed lines) in Figure 10. The effect of coupling becomes very obvious and the matching between the data and numerical results is pretty good. Small peaks, located at the resonance frequencies of the other inlet, are evident when both inlets are present and disappear for artificially closing the adjacent inlet. These small peaks are located at the frequencies corresponding to the resonance modes of the other inlet and mimic the peaks found in the observed amplification functions.

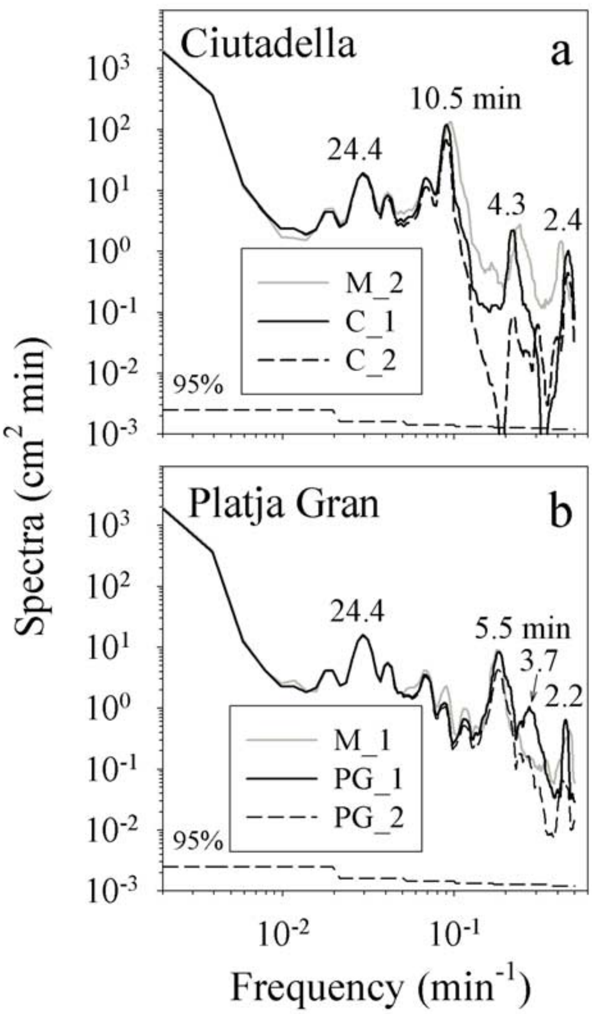


**Figure 9.** Computed sea level spectra at Ciutadella (a), and Platja Gran (b), for a point located near the end of the inlet (solid line) and near the middle (dashed line). Measured spectra for positions M_1 and M_2 are also included (in gray) for better comparison.

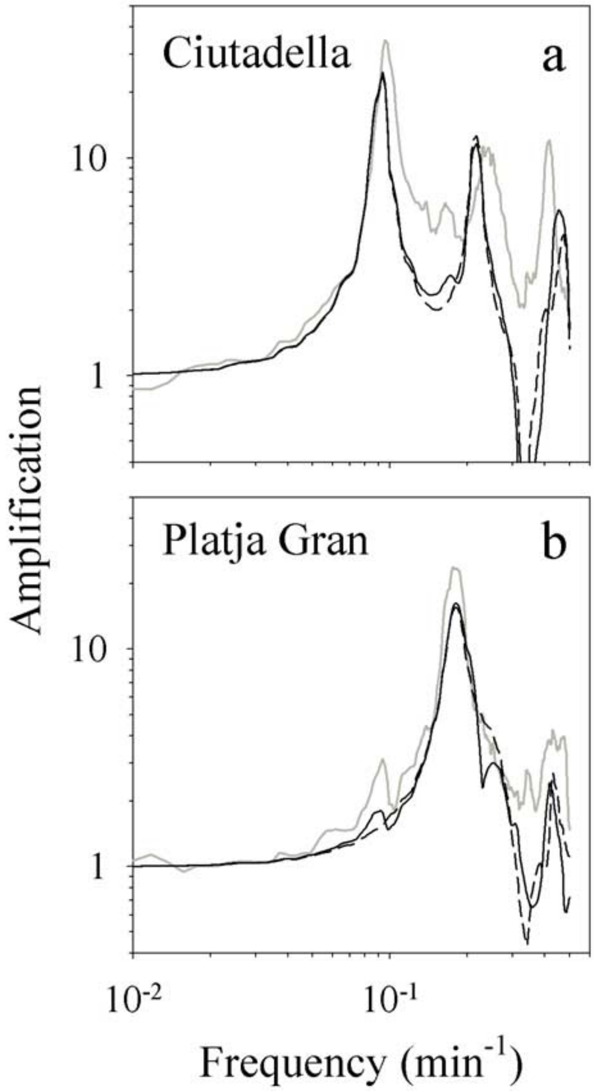


**Figure 10.** Amplification factors computed by using the numerical model for Ciutadella (point C_1) (a) and Platja Gran (point PG_2) (b) with the presence of both inlets (solid lines) and artificially closing the adjacent inlet (dashed lines). Measured amplification factors for positions M_1 and M_2 are also shown (in gray) for better comparison.

## 5. Concluding Remarks

[31] On the basis of the field evidences a simple linear wave theory has been constructed to investigate the resonance coupling of two adjacent inlets. The results explain well the fundamental features of the coupled inlet responses. The theory also reproduces the main features of the field observations at Ciutadella and Platja Gran inlets, Menorca Island, Western Mediterranean. However, owing to the simplifications of bathymetry and shoreline configuration in the analytical solutions some disagreement is found con-

cerning the magnitudes for peak responses and the resonance frequencies. A numerical model based on the linear shallow water equations is also used to simulate the inlet responses using the real bathymetry and topography. The numerical solutions agree with the field observation very well.

[32] The analytical model also demonstrates that resonant responses could be significantly amplified if the inlet length becomes very close to each other. This is an important feature if the coupled inlet system is used as a device for wave energy generation.

[33] For the low energetic wave conditions studied in the paper the linear wave theory is adequate, even for the resonance condition. However, for a "rissaga" event, the incident wave energy level and the inlet responses are much larger, reaching wave heights inside the inlets of several meters. The nonlinearity becomes then very important. The coupling mechanism becomes complex and more interesting because of the generation of superharmonics and subharmonics, which might coincide with the resonance mode of neighboring inlet. The investigation of this problem is underway.

[34] **Acknowledgments.** This work has been carried out during the visit of one of the authors (P.L.) at IMEDEA, as a "Profesor Visitante Iberdrola de Ciencia y Tecnología." The research is also partly supported by National Science Foundation Grants (BES 9714182 and CMS 9908392) to Cornell University. CICYT- CYTMAR MAR95-1863 project provided the necessary funding for the acquisition of the data. The authors would like to thank R. Medina, I. Losada, C. Vidal, and F. Martín from the Ocean and Coastal Research Group at the University of Cantabria for kindly providing the numerical model used in this study and for their collaboration on the design and developing of LAST-97 measurements in Ciutadella region. Finally, the inestimable help from local people at Ciutadella when deploying the instruments in LAST-97 is sincerely acknowledged.

## References

Aida, I., T. Hatori, M. Koyama, H. Nagashima, and K. Kajiura, Long-period waves in the vicinity of Onagawa Bay (I)—Field measurements in Onagawa and Okachi bays, *J. Oceanogr. Soc. Jpn.*, *28*, 207–219, 1972.

Arai, K., and Y. Tsuji, Lack of excitation by tsunamis of normal modes of sea-surface oscillations in bays, *Pure Appl. Geophys.*, *151*, 161–181, 1998.

Emery, W. J., and R. E. Thomson, *Data Analysis Methods in Physical Oceanography*, 634 pp., Pergamon, New York, 1997.

Gomis, D., S. Monserrat, and J. Tintoré, Pressure-forced seiches of large amplitude in inlets of the Balearic Islands, *J. Geophys. Res.*, *98*, 14,437–14,445, 1993.

Grupo de Ingeniería Oceanográfica y de Costas (GIOC), The H2D long wave propagation model (in Spanish), Internal Rep., 120 pp., Univ. of Cantabria, Cantabria, Spain, 1990.

Mei, C. C., *The Applied Dynamics of Ocean Surface Waves*, 740 pp., World Sci., River Edge, N.J., 1989.

Monserrat, S., A. Ibbetson, and A. J. Thorpe, Atmospheric gravity waves and the "rissaga" phenomenon, *Q. J. R. Meteorol. Soc.*, *117*, 553–570, 1991.

Monserrat, S., A. B. Rabinovich, and B. Casas, On the reconstruction of the transfer function for atmospherically generated seiches, *Geophys. Res. Lett.*, *25*, 2197–2200, 1998.

Murty, T. S., *Seismic Sea Waves—Tsunamis*, Bull. 198, 337 pp., Fisheries Res. Board of Canada, Ottawa, 1977.

Nakano, M., The secondary undulations in bays forming a coupled system, *Proc. Phys. Math. Soc. Jpn.*, *3*, 372–380, 1932.

Nakano, M., and N. Fujimoto, Seiches in bays forming a coupled system, in *Tsunamis–Their Science and Engineering*, edited by K. Iida and T. Kawasaki, pp. 339–358, Terra Sci., Tokyo, 1983.

Rabinovich, A. B., and S. Monserrat, Generation of meteorological tsunamis (large amplitude seiches) near the Balearic and Kuril islands, *Nat. Hazards*, *18*, 27–55, 1998.

Rabinovich, A. B., S. Monserrat, and I. V. Fine, Numerical modeling of extreme seiche oscillations ("rissaga waves") in the vicinity of the Balearic Islands, *Oceanology*, *39*, 12–19, 1999.

Tintoré, J., D. Gomis, S. Alonso, and D. P. Wang, A theoretical study of large sea level oscillations in the Western Mediterranean, *J. Geophys. Res.*, *93*, 10,797–10,803, 1988.

Wilson, B., Seiches, *Adv. Hydrosci*, *8*, 1–94, 1972.

P. L.-F. Liu, Cornell University, Hollister Hall 220, Ithaca, NY 14853, USA. (pll3@cornell.edu)

M. Marcos, GOIFis (IMEDEA), C/Miguel Marques, 21, 07190, Esporles, Illes Balears, Spain. (marta.marcos@uib.es)

S. Monserrat, Departament de Física, Universitat de les Illes Balears, 07071 Palma de Mallorca, Spain. (s.monserrat@uibes)

A. Rabinovich, P. P. Shirshov Institute of Oceanology, 36 Nakhimovsky Prosp., 117851 Moscow, Russia. (abr@iki.rssi.su)